RSC Advances

PAPER

View Article Online
View Journal | View Issue

Cite this: *RSC Adv.*, 2023, **13**, 4495

Improved chemometric approach for XRF data treatment: application to the reverse glass paintings from the Lipari collection

Francesco Armetta,[a] Maria Luisa Saladino,[a] Maria Clara Martinelli,[b] Rosario Vilardo,[b] Gianfranco Anastasio,[c] Sebastiano Trusso,[d] Viviana Mollica Nardo,[d] Dario Giuffrida *[de] and Rosina Celeste Ponterio[d]

The Aeolian cultural heritage preserves hundreds of testimonies of the past that have passed through six millennia of history. Among these, the Archeological Park of the Aeolian Islands with the Museum Luigi Bernabò Brea (Italy) preserves a valuable set of artworks, which are related to a little-known 'popular' figurative heritage. It is an assemblage of small glass foils decorated using the technique of reverse painting, datable to between the end of the 17th century and the end of the 18th century, and actually under investigation by historians. Here, an X-ray fluorescence (XRF) spectroscopy study (performed with portable equipment) is combined with a multivariate approach that allows us to define the best way to process the data to detect compositional differences and similarities among the glass supports. The Principal Component Analysis (PCA) and Hierarchical Cluster Analysis (HCA) were applied both on normalized spectra and on normalized peak areas in order to establish the chemometric approach with the highest grouping ability. Results showed that the analysis of the normalized area provides the most reliable grouping based on the different elemental compositions, without problems coming from the background or peak-shape distortions. The obtained results can be used by researchers involved in the analysis of XRF data as a guideline to perform chemometrics. Furthermore, regarding the reverse glass, they can be divided into different typologies based on composition differences, providing a further discrimination criterion for historians involved in the study of the collection to determine the provenance and dating of the items.

Received 22nd December 2022
Accepted 3rd January 2023

DOI: 10.1039/d2ra08178d

rsc.li/rsc-advances

1 Introduction

The Aeolian cultural heritage preserves hundreds of testimonies of the past that have passed through six millennia of history in a wide variety of forms and cultural expressions. Alongside its more distinctive archaeological asset, the Museum Luigi Bernabò Brea of the Archeological Park of Aeolian Islands (Italy)[1] preserves a valuable set of artworks, which are related to a little-known 'popular' figurative heritage.[2] It is an assemblage of small glass foils decorated using the technique of reverse painting, datable to between the end of the 17th century and the end of the 18th century. The collection was gradually built up by L. Bernabò Brea and M. Cavalier between the 1950s and the 1970s, gathering specimens from private collections of families from the Aeolian islands and then donated to the Museum. The number of specimens further grew in the following years thanks to donations from citizens. Between December 19th 2009 and April 18th 2010, the materials were the subjects of a first temporary exhibition, *Miracula in vitro*,[3] held in the Church of Santa Caterina in Lipari.[4]

The provenance of the artworks is so diversified that it is not possible to draw, only on stylistic analysis, a common reference framework: it seems that some specimens were the result of exchanges with sailors and traders from northern and central Italy, a testimony of how this archipelago had always been a crossroads of the Mediterranean throughout the centuries; nevertheless, local Aeolian production of painted glass has also been hypothesized on the basis of evidence.

The painting technique (known as reverse painting on glass foils, painting under glass, painting behind glass or cold painting on glass) is considered one of the highest forms of Italian popular culture with different schools spread all over Italy, each one characterized by well-defined peculiarities.[5] The method consists of the cold application of an oil or tempera

[a]*Dipartimento di Scienze e Tecnologie Biologiche Chimiche e Farmaceutiche (STEBICEF) and INSTM-Palermo, Università degli studi di Palermo, Viale delle Scienze, Ed.17, I-90128 Palermo, Italy*

[b]*Museo Archeologico Luigi Bernabò Brea, Via Castello, 2, I-98050 Lipari, Messina, Italy*

[c]*Museo Regionale delle Tradizioni silvopastorali di Mistretta, Via della Libertà 184, 98073 Mistretta, Italy*

[d]*IPCF-CNR, Istituto per i Processi Chimico Fisici, V.le F. S. d'Alcontres 37, 98158 Messina, Italy. E-mail: dario.giuffrida@ipcf.cnr.it*

[e]*Dipartimento di Civiltà Antiche e Moderne, Università degli Studi di Messina, Polo Annunziata, Via A. Giuffré, 98168, Messina, Italy*

layer on the back side of a glass foil, and the images then are specular with respect to the way they appear on the front side. Such a method forces the artist to visualize the whole painting structure in advance and to apply the colors in an inverse chronological order with respect to traditional painting (from the foreground to the background/from the details to the

Fig. 1 Selection of glass paintings: A: inv. 26008; B: inv. 26009; C: inv. 26015; D: inv. 26003; E: inv. 26014; F: inv. 26030; G: inv. 26017; H: 26034; I: inv. 26021; J: inv. 260112. Archaeological Museum of Lipari, Aeolian Islands, Messina.

general). This is a method that leads often to the total absence of perfectionism.[6] On the one hand, this method is very tough because of the reverse order of application of the colors. On the other hand, the glass substrate makes it possible to copy the image from a paper template; paper prints devoted to reverse glass paintings were, in fact, very popular, allowing serial production to some extent. This led to the identification of stylistic similarities among paintings, even those done in different workshops. Other template models were xylography, chalcography and zincography. These models, in turn, represent devotional images of eighteenth-century production by the Remondini, publishers and printers from Bassano whose works were widespread throughout Europe.[7] For the oldest images, the influence of the pictorial production of the 15th and 16th centuries is not excluded. The figurative repertoire includes sacred iconographies drawn from *Miracula Picta* and biblical scenes[8] (Fig. 1): in more detail, about half of the objects of the museum collection are typical Marian iconography examples, while the remaining are dedicated to one or more saints (St. Joseph, St. Anne, St. Francis of Paola, St. Michael the Archangel, St. Filomena, and the Holy Family), biblical episodes connected to the Old or New Testament (the Judgment of Solomon, the Nativity, the Adoration of the Shepherds, the Adoration of the Magi, the Martyrdom of St. John the Baptist) and hagiographies (the Martyrdom of St. Bartholomew). Four specimens that represent the Annunciation scene represent as many different stylistic features that have been recognized within this production in the period between the end of the 18th century and the end of the 19th century.

With respect to their function, the main assumption is that they have a dual propitiatory and apotropaic function, from which those within the domestic sphere get comfort, or at least protection. In fact, they were placed at the bedside in the master bedrooms, or placed in the house's common spaces. The specimens of Museum L. Bernabò Brea have, thus, a double anthropological and historical-artistic value; the first one is related to the knowledge of traditional Sicilian culture linked to religiosity and forms of domestic devotion,[9,10] while the second one is related to technical aspects of this peculiar pictorial technique in southern Italy and Sicily. From this point of view, the reverse paintings of the museum collection could trace the circulation of these objects within the Mediterranean during the 18th and 19th centuries: as already mentioned, alongside specimens of local production and coming from Southern Italy workshops, the collection in fact includes specimens – the oldest – that are characterized by influences from the Venetian school.

1.1 Historical and stylistic classification

The collection, preserved at the Museo Archeologico Luigi Bernabò Brea in Lipari, consists of 31 items. A tentative classification was proposed solely on a stylistic basis. Some items show influences of Neapolitan, Apulian and Venetian workshops, while the majority show features characteristic of Sicilian production. There are some paintings whose origin is impossible to hypothesize on only a stylistic basis.[9] The hypothesis of a local tradition of production of glass reverse painting is attested by an image of an engraving present in the book by the Archduke Louis Savior of Austria Die Liparischen Inseln,[11] in the volume dedicated to Filicudi. Here, in a typical home interior of Chianu or Puortu, belonging to a peasant, at least six paintings on glass hanging on a wall of the house, recognizable by the typical glove box frames, can be seen. A further element in favor of a local pictorial practice is the presence of numerous paintings on glass throughout the Aeolian archipelago and also in the Tyrrhenian province of Messina, the result of artisans from Lipari, Stromboli, and Filicudi, who keep on painting on glass until the mid-1960s. One of the most important references for dating the figured Aeolian glasses is the collection preserved in Salina at the Sanctuary of the Madonna del Terzito, which turn out to be the only datable specimens. Nevertheless, a classification based on the material characterization, which can be used to support or refute the hypotheses advanced on historical and stylistic grounds, is still missing.

1.2 Composition analysis

Chemical composition data can provide information about the kind of glass and the type of raw materials employed in its production,[12] for example, the amount of sodium or calcium can easily differentiate soda-lime glasses. The determination of major, minor, and trace elements can be performed using several analytical techniques able to quantify the analytes with a different sensibility. Inductively Coupled Plasma Mass Spectrometry (ICP-MS) offers fast, multi-elemental, trace level, quantitative analysis but needs a small amount of sample to be destroyed.[13] In the field of cultural heritage analysis, often conservators do not give approval to damage the artifact, and this is a strong limitation of the use of this technique. It was demonstrated that the combination of ICP-MS with a laser ablation tool provides good results for the quantification of the elements contained in a collection of archaeological glasses.[14,15] Even if these promising results seem to indicate a solution, the use of laser ablation is still micro-destructive and not suitable at all for the investigation of glasses at the museum. In this view, XRF investigation performed by portable equipment has found a relevant place in the analysis of objects of artistic interest, thanks to the advantages of non-invasiveness and the possibility to perform the measurement directly at the museum or in the place where the sample is exposed or stored. As a function of the kind of matter under investigation, portable XRF can provide semi-quantitative measurements[16–18] or quantitative with standards' calibration[19,20] with a limitation on the depth information.[21] In the case of an investigation on a large collection of similar objects, this limit can be overcome by the consideration that matrix effects, mainly coming from fluorescence radiation absorption with the sample matrix, do not strongly influence the elemental fluorescence and that a simple spectra comparison can be enough to highlight differences and similitudes.[22] Moreover, recently, several chemometric tools have been developed and applied to XRF data to aid in the data analysis and thus increase the potential of the technique.[23–26]

Multivariate processing can be applied both on raw spectra and the extracted information on elemental composition,[27,28] but there are no guidelines or detailed studies exploiting the best way to perform the data analysis. In this study, the investigation of the Lipari glass collection by XRF measurements allowed us to tailor and evaluate the best chemometric approach to unveil the composition differences and, hence, differentiate and group the glasses.

2 Methods

The XRF measurements were performed *in situ* by placing a portable spectrometer, Tracer III SD Bruker AXS, in contact with the surface of the front side of the 31 glasses. For each glass, three spots were analysed – in the lower, middle, and top areas – to check the homogeneity and improve the statistics of the data. The spectrometer source is a rhodium target X-ray tube operating at 40 kV and 11 mA, with an acquisition time of 30 seconds. The detector is a 10 mm^2 silicon drift X-Flash with Peltier cooling system and a resolution of 145 eV at 100 000 cps. The S1PXRF software manages data acquisition. The spectral assignment of the characteristic peaks of an element was carried out using the database contained in the ARTAX 8 software, which also permits us to perform the integral intensity calculation of the different spectral lines through Bayes deconvolution. In each spectrum, the signals of rhodium (Rh) and argon (Ar), due to the source and the atmosphere, respectively, are present. As an example, the XRF spectrum of fragment 4 is reported in Fig. 2.

The spectra were preprocessed before applying Hierarchical Cluster Analysis (HCA) and Principal Component Analysis (PCA), obtaining two sets of data. In the first set, we considered the spectra data normalized to the intensity of the Si peak at 1.74 keV because Si is expected to represent the glass bulk, while other elements are due to production additives that are used at much lower concentrations (the same approach was used by some of us previously [22]). For the second set, the net area percentages of the identified elements were estimated from each spectrum. The K_α peak was considered for the elements silicon (Si), sulfur (S), potassium (K), calcium (Ca), chlorine (Cl), titanium (Ti), manganese (Mn), iron (Fe), copper (Cu), nickel (Ni), arsenic (As), gallium (Ga), rubidium (Rb) and strontium (Sr), while the $L_\alpha 1$ peak was considered for the evaluation of lead (Pb). Net peak area values were obtained after peak deconvolution and background subtraction procedures. Finally, each spectrum was normalized with respect to its total area. (Rh and Ar contributions were estimated in the deconvolution procedure in order to avoid inaccuracies in case of overlapping signals as in the case of the presence of the chlorine (Cl) peak; their values were excluded from the analysis as they do not provide any useful information about the glass composition). Results were then analysed through a chemometric approach. Thus, after an overall data observation, the Principal Component Analysis (PCA) and the Hierarchical Cluster Analysis (HCA) were applied, both to the normalized spectra and the net area percentage values, using the software Past 4.05.[29] The PCA procedure on the spectra was performed in the energy range between 2.00 and 16.00 keV, because all emissions of identified elements fall in this range, and, considering a 0.02 keV energy step, a matrix size of 93 × 701 was obtained. The PCA procedure performed on the net area percentage values allowed the preparation of a smaller matrix, 93 × 15 in size. The discriminant analysis (sometimes called canonical variate analysis) was performed after the assignment of the group and enabled us to confirm the difference between the hypothesized groups. The exact number of clusters into which the glasses should be classified was set up as a parameter *a priori* so that HCA after the PCA procedure was performed by changing the number of clusters. The most reliable results were obtained when the classification was performed with seven clusters.[30]

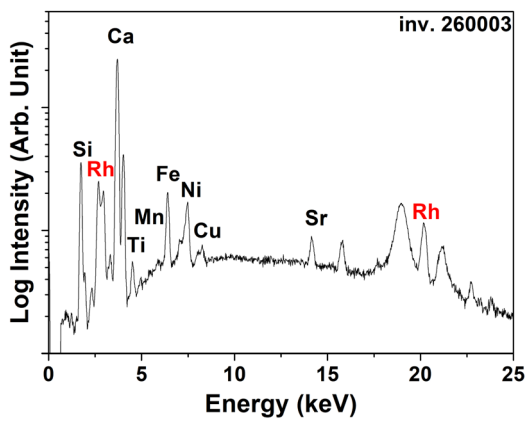

Fig. 2 XRF spectrum of reverse glass inv. 260003. In the XRF spectrum, the labels indicate the K emission lines of the elements.

3 Results and discussion

All the spectra show similar peak profiles with intense signals of calcium (Ca) and low signals of silicon (Si), sulfur (S), potassium (K), chlorine (Cl), titanium (Ti), iron (Fe), nickel (Ni), gallium (Ga), rubidium (Rb) and strontium (Sr), identified in each spectrum. In contrast, signals of copper (Cu), manganese (Mn), arsenic (As) and lead (Pb) are present only in some glasses. Nothing can be declared about the presence of sodium because it cannot be identified with the experimental conditions used for the data acquisition. Some elements show large variations from glass to glass with respect to others. For example, the area variations for the Si, Cl, Ga, S, Ti, Fe, Rb, and Ni peak areas are almost within the 25^{th} and 75^{th} percentiles (Fig. 3).

In contrast, emissions from As, Ca, Cu, K, Mn, and Pb show the presence of some outliers making these elements characteristic for the discrimination of the corresponding glasses that strongly differ in manufacturing and/or provenance from the glasses with a composition distribution inside the interquartile range. It is interesting to note that for As, Cu, Mn and Pb the mean value is close to zero, while, for the outliers, the area reaches significant percentage values, indicating that the outliers are glasses from different manufacturing processes compared to the others. The results of the PCA procedure performed on the normalized spectra are reported in Fig. 4. The

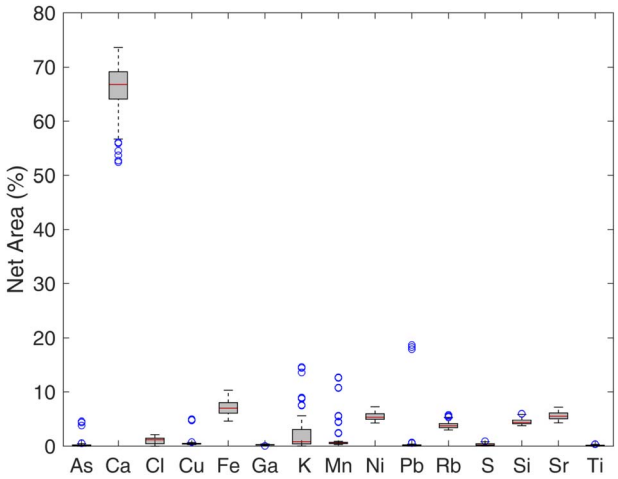

Fig. 3 Box plot of the intensity of the XRF emission lines. Lower and upper box boundaries are the 25th and 75th percentiles, respectively. Line inside box is the median, and the lower and upper error lines are the 10th and 90th percentiles, respectively. Circles are data with values further than 1.5 times the box height from the box boundaries.

scores of the first four components (PC1–PC2 plane Fig. 4a, PC3–PC4 plane Fig. 4b) explain the 93.2% of the total variance. The clusters resulting from the HCA procedure are identified in the plots by different colors. In the PC1–PC2 plane (Fig. 4a) a group, including 6 out of 7 clusters, extends along the PC1 direction, while a cluster characterized by a large variance along the PC2 axis incorporates only three spectra. Fig. 5 shows the loadings as determined by the PCA. As can be seen, each PC is related to well-defined XRF signals coming from different elements. Ca, Pb, K and Mn XRF peaks, in fact, are the main features that characterize the first four PCs, while smaller features related to Fe and Cu are present. The high score values of the PC2 component observed for glass #26015 thus indicate the presence of a high content of Pb, corresponding to the outliers observed in the Pb box plot in Fig. 3. The distribution along PC1 observed in Fig. 4a for the majority of the glasses is then due to Ca peak intensity variations; being the most intense peak in the XRF spectra its variation leads to the almost continuous spread of the scores along the PC1 axis.

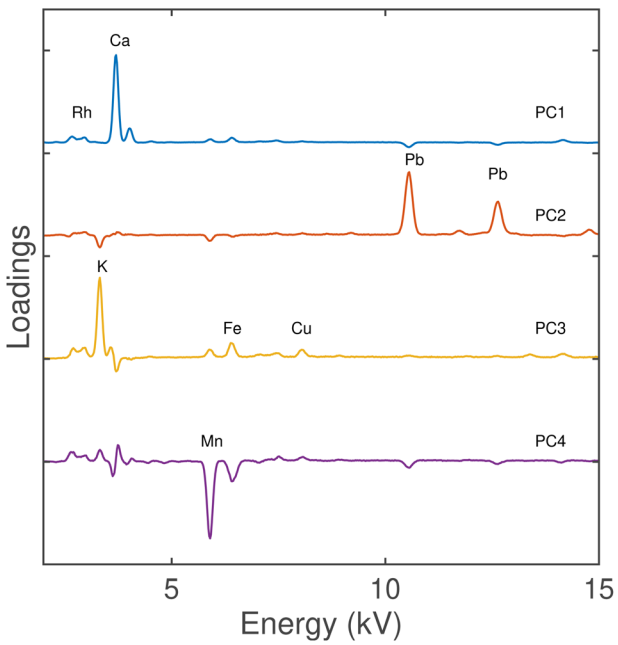

Fig. 5 Loadings of the four PCs computed on the normalized spectra dataset.

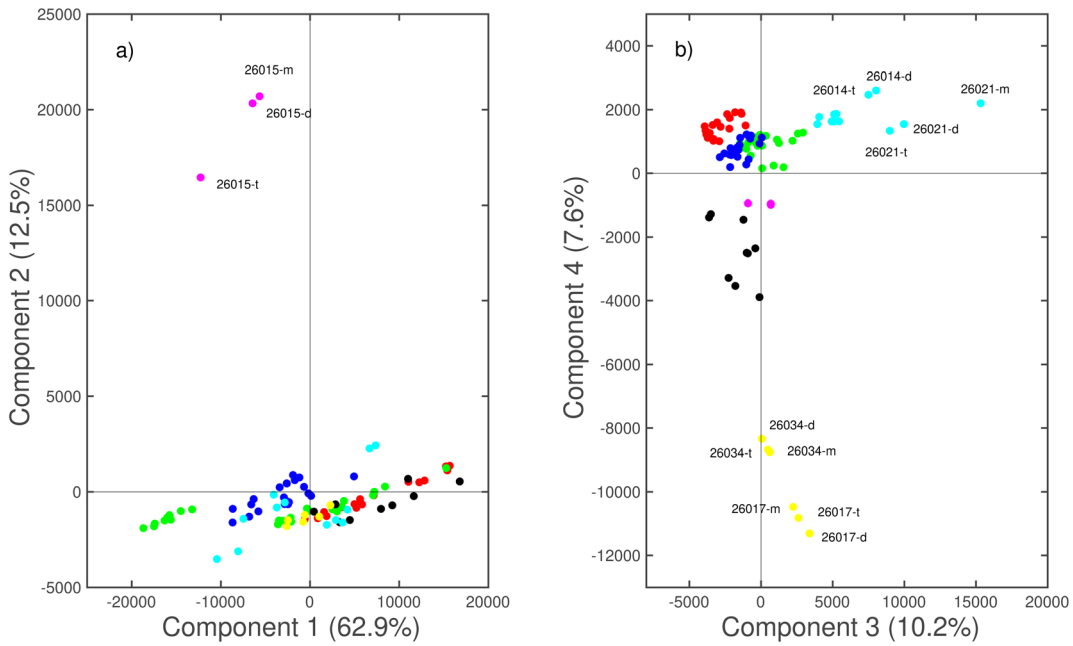

Fig. 4 Projection of principal components PC1 *vs.* PC2 (a) and PC3 *vs.* PC4 (b) computed on the normalized spectra dataset.

The observation of the PCA scores in the plane PC3–PC4 (even if accounting for an amount of 17.8% of the total variance) can give further information about the glasses' chemical composition. Most of the glasses are grouped in the upper-left quadrant with negative PC3 and positive PC4. The possible outliers are located at positive PC3 values (identified as #26014 and #26021 glasses) and negative PC4 values (#26017 and #26034 glasses).

As reported above, the loadings plot shows the PC3 dependence on the K, Fe, and Cu contents, while PC4 depends on the Mn content. Therefore, the two clusters can be identified by some specific elements: the light blue cluster with the presence of K, and the yellow cluster with the presence of K and/or Fe and Cu (unfortunately it is difficult to discriminate between the three contributions). The main cluster in the second quadrant was divided into three sub-clusters on the basis of the PC1, and then on the Ca peak contribution: low (green), middle (blue), and high (red).

It is worth emphasizing that all the PCs are influenced in a different way by the peak related to the different elements and these contributions are not discriminated. A confirmation of the classification was made by Ward's HCA of the normalized spectra (Fig. 6). The clusters are joined such that the increase in within-group variance is minimized. It is a bit daunting to observe that, in many cases, the spectra acquired on the same glass are far; moreover, the identification of well-defined clusters is not reliable at all. There are no specific rules about the determination of a correct limit-distance. In our case, fixing a low limit could probably separate some of the clusters identified through PCA and especially the probable outliers (#26017, #26034, #26021, and #26015), but some clusters are mixed. Furthermore, looking at the dendrogram separation, the clusters' similitude seems to not agree with the classification obtained after performing the PCA, with the main cluster comprised of red, blue, and green sub-clusters. Despite the good amount of obtained information about the influence of some elements on glasses' differentiation, the analysis of the spectra does not provide a good classification due to the ubiquitous contribution of source signals on the variance and of the high difference in intensity between the peaks of Ca and Pb, which strongly affect the highest amount of explained variance. For this reason, here we proposed a different way to analyse the XRF data, based on the net area percentage of the peaks of the elements constituting the glass, highlighting the relationship between the elemental composition and the glasses' classification. (Fig. 7a and b), two-dimensional scatter plots or maps of scores used to interpret properties of the samples (scores plot,

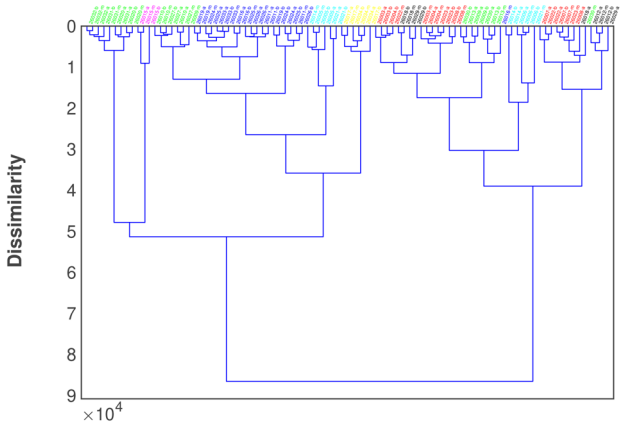

Fig. 6 Dendrogram of Ward's HCA clustering on the normalized spectra.

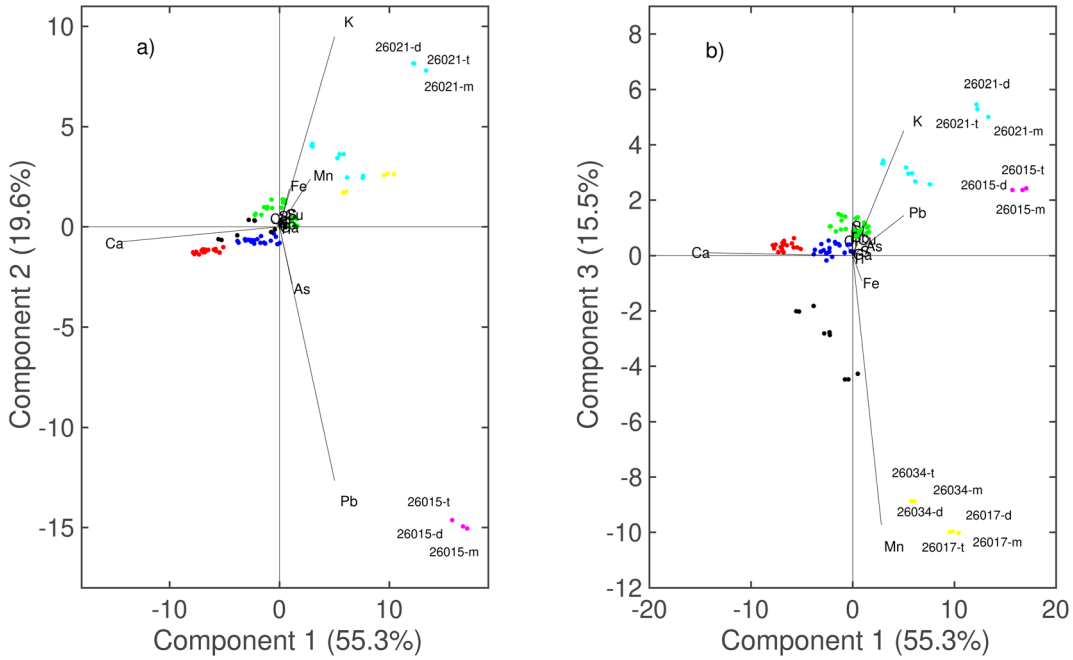

Fig. 7 Projection of principal components PC1 *vs.* PC2 (a) and PC1 *vs.* PC3 (b) computed on the net area% dataset.

point-measurements distribution, or elemental peak area in this case) with the variables' properties (X-loadings, elemental distribution), clearly display simultaneously the samples' similitude and the relationship of the variables. A high number of variables make the biplots confusing; for this reason, one was not plotted for the PCA of the spectra. The PCA scores in the PC1–PC2 plane (Fig. 7a) and PC1–PC3 plane (Fig. 7b) explain the 90.4% of the total variance. In this case, the variance is better distributed among the first component, and also the variables influencing the loading are more balanced, therefore we observe a wider distribution of the scores into the plane of the three PCs considered. The biplot of the first two PCs clearly shows the influence of Pb on the discrimination of glass #15 and the ones of K on the sample #26021, while the use of PC3 enhanced the influence of Mn for the discrimination of glasses #26017 and #26034. Also, in this case, it is possible to identify a cluster of samples strongly influenced by K (light blue) and one cluster of glasses that is slightly influenced by Mn (yellow).

It is possible to identify a main cluster that can be divided into three sub-clusters on the basis of the Ca influence (red, blue, and green on decreasing the Ca area), but, thanks to the PC2, it is possible to improve the description of the green cluster, which is located at positive values due to the effect of K loading. The HCA of the net area% (Fig. 8) is in perfect accordance with the classification obtained after performing the PCA.

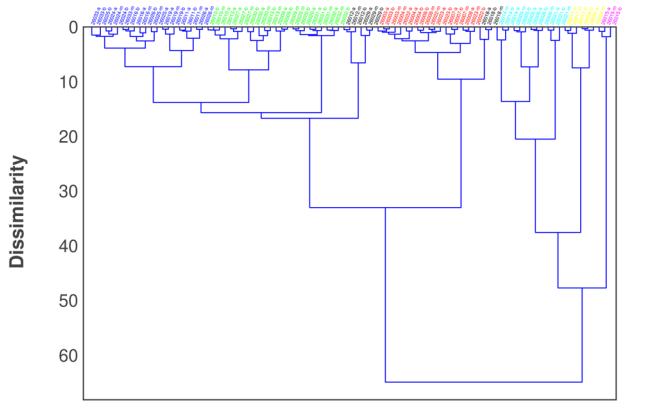

Fig. 8 Dendrogram of Ward's HCA clustering on the net area% dataset.

Moreover, it is possible to observe that the possible outliers (and their clusters) are located on one side of the dendrogram and that the red, blue, and green clusters are similar to each other and they are part of the main cluster. The location of the black cluster close to the red one is not so strange considering that these objects are closer to the red cluster than the yellow one in the PCA.

In this case, the objects of the same glass are close to each other, and anomalies are not recognized. The results of the linear discriminant analysis (LDA) method computed using 5 principal components are reported in Table 1. The method recognizes the seven groups with the highest prediction ability (total 100.0% ability).

4 Discussion

The chemometric tools provided different results as a function of the analysed data form. The analysis of the normalized spectra:

- was affected by the influence of source signals that affect loadings of the first PCAs.
- was influenced by the large difference in peak intensity, which increases the contribution of a variable on loading.
- was influenced by the convolution of close emission bands.
- made the loading interpretation difficult because of the simultaneous effect of several peaks on the PC.

On the contrary, the analysis of the net area:

- excluded any effect of source signals.
- reduced the difference between elements making the variance between variables more balanced.
- excluded any mistakes due to the convolution of the peaks, because it was based on a deconvolution for the estimation of the peak area.
- permitted the preparation of biplots for a fast and easy interpretation of the results.
- provided an easy and confident comparison with other chemometric approaches, *i.e.*, HCA.

All these features strongly influence the quality classification of the object and the best results can be obtained by the analysis of the net area%. Regarding the investigation of the collection of reverse paintings, it is possible to observe that the main cluster comprised of red, blue and green objects is characterized by a similar and simple composition, which is supposed to

Table 1 Confusion matrix resulting from LDA with five principal components

	Predicted group							
Given group	Red	Green	Black	Light blue	Yellow	Blue	Magenta	Total
Red	18	0	0	0	0	0	0	18
Green	0	24	0	0	0	0	0	24
Black	0	0	9	0	0	0	0	9
Light blue	0	0	0	12	0	0	0	12
Yellow	0	0	0	0	6	0	0	6
Blue	0	0	0	0	0	21	0	21
Magenta	0	0	0	0	0	0	3	3
Total	18	24	9	12	6	21	3	93

have the same origin based on the comparison with already assigned reverse glass paintings[22] and, considering the location of the museum, it could be reasonable that they are coming from Sicily where usually glasses show a low Fe content and are fired using soda lime.[31] In light of the other clusters, the presence of elemental outliers can drive the assignment. The light blue and yellow clusters could come from Veneto and, in general, from northern regions, because all of them show a low Fe content and the presence of Mn, usually used to make the glass transparent. The light blue cluster is characterized by the presence of a high amount of K, which is detrimental to the use of potash as the firing agent, while, for the other glasses, Na was used as the firing agent, even if Na cannot be detected by XRF measurements. Nevertheless, differences in the use of the firing agent can hardly be used to determine the production period and geographical area. The two different fluxing materials, in fact, were used in the same geographical area. The magenta cluster characterized by one reverse painting mainly differs from the others in the Pb content, which is usually used to color the glass depending on the raw minerals, even in combination with other minerals.[32,33] On the other hand, lead oxide (PbO) can also be used to weaken the network and lower the melting temperature of the glass during its preparation.[34] It is interesting to note that this glass was the only one assigned to Palermitan manufacturers on a stylistic basis.

5 Conclusions

XRF data of a glass collection from Lipari Museum were processed by multivariate analysis by means of PCA and HCA. Processing of the spectra and integrated peaks provides different results and the comparison allowed us to critically define the best protocol to apply chemometric tools on this kind of data. In detail, the analysis of the normalized area provides the most reliable grouping based on the different elemental composition, without problems coming from the equipment or environmental influences. The proposed approach not only provides a better way to perform chemometric analysis on XRF data using portable equipment, but also permits the grouping of reverse-painted glasses based on the compositional description. It is interesting that, even if not quantitative, this approach provides a formidable tool to finely distinguish between glasses belonging from a wide collection.

Author contributions

MLS and RCP: conceptualization and methodology, funding, editing. VMN and FA: XRF data acquisition. ST and FA: XRF data treatment, writing–review and editing. DG, RV and MCM: historical investigation. All authors contributed to the article and approved the submitted version.

Conflicts of interest

The authors declare that they have no competing interests.

Acknowledgements

F. A. thanks MIUR for the Project PON Ricerca e Innovazione 2014–2020 – Avviso DD 407/2018 "AIM Attrazione e Mobilità Internazionale" (AIM1808223). This study was carried out in the framework of the Scientific Agreement between IPCF-CNR, the Department STEBICEF of the University of Palermo, and the Archeological Park of Aeolian Islands.

Notes and references

1 **https://www.beniculturali.it/luogo/museo-archeologico-regionale-eoliano-luigi-bernabo-brea**.
2 A. Buttitta, *La pittura su vetro in Sicilia*, Sellerio, 1972.
3 **https://www.culturaitalia.it/opencms/it/contenuti/eventi/event_2029.html**.
4 M. A. R. Eoliano, *Miracula in vitro: pitture su vetro dal secolo 18. al 19: collezione Bernabò Brea-Cavalier, testi Michele Benfari, Sergio Todesco, Barbara Brundu, Agata Polizzi ; fotografie di Giuseppe MineoMuseo regionale archeologico eoliano "L. Bernabò Brea", Lipari*, 2009.
5 G. Funaro and R. Rivelli, *Vetri dipinti italiani*, Ceam, 1998.
6 G. D'Agostino, Arte popolare in Sicilia. *Le tecniche, i temi, i simboli*, Flaccovio, Palermo, 1991.
7 C. A. Zotti-Minici, *Le stampe popolari dei Remondini*, Neri Pozza, Vicenza, 1994.
8 A. Uccello, *Pitture su vetro del popolo siciliano, Ente Provinciale per il Turismo*, Siracusa, 1968.
9 S. Todesco, *Archivio Storico Messinese, 1993, 64(1993), 95–142, poi ristampato in Id. (a cura di), Atlante dei Beni etno–antropologici eoliani, Palermo, Assessorato Regionale BB.CC.AA. e P.I*, 1995.
10 F. Riccobono and F. Sarica, *Immagini devote in Sicilia*, Edas, Messina, 1982.
11 L. Salvator, *Herzherzog von Österreich, Die Liparischen Inseln, Fünftes heft, Filicuri*, Druck und Verlag von Heine Mercy, Prag, 1985.
12 D. C. W. Sanderson, J. R. Hunter and S. E. Warren, *J. Archaeol. Sci.*, 1984, **11**, 53–69.
13 E. Caponetti, F. Armetta, L. Brusca, F. D. Chillura, M. L. Saladino, S. Ridolfi, G. Chirco, M. Berrettoni, P. Conti, B. Nicolò and S. Tusa, *Microchem. J.*, 2017, **135**, 163–170.
14 M. Bertini, A. Izmer, F. Vanhaecke and E. Krup, *J. Anal. At. Spectrom.*, 2013, **28**, 77.
15 P. Weis, M. Dücking, P. Watzke, S. Mengesa and S. Beckera, *J. Anal. At. Spectrom.*, 2011, **26**, 1273.
16 P. J. Potts, A. T. Ellis, P. Kregsamer, J. Marshall, C. Streli, M. West and P. Wobrauschek, *J. Anal. At. Spectrom.*, 2004, **19**, 1397–1419.
17 M. Ganio, S. Boyen, T. Fenn, R. Scott, S. Vanhoutte, D. Gimeno and P. Degryse, *J. Anal. At. Spectrom.*, 2012, **27**, 743.
18 E. Caponetti, F. Armetta, F. D. Chillura, M. L. Saladino, S. Ridolfi, G. Chirco, M. Berrettoni, P. Conti, B. Nicolò and S. Tusa, *Mediterr. Archaeol. Archaeom.*, 2017, **17**, 11–18.

19 S.-M. Lim, Y.-S. Kwon, Y.-R. Cho and W.-S. Chung, *J. Conserv. Sci.*, 2021, **37**, 451–463.
20 A. G. Karydas, *Ann. Chim.*, 2007, **97**, 419–432.
21 A. Gianoncelli and G. Kourousias, *Appl. Phys. A*, 2007, **89**, 857–863.
22 V. Renda, V. Mollica Nardo, G. Anastasio, E. Caponetti, C. Vasi, M. Saladino, F. Armetta, S. Trusso and R. Ponterio, *Spectrochim. Acta, Part B*, 2019, **159**, 105655.
23 C. Scatigno, N. Prieto-Taboada, C. García-Florentino, S. F.-O. de Vallejuelo, M. Maguregui and J. M. Madariaga, *Environ. Sci. Pollut. Res.*, 2018, **25**, 6285–6299.
24 C. Scatigno and G. Festa, *Microchem. J.*, 2021, **171**, 106863.
25 V. Panchuk, I. Yaroshenko, A. Legin, V. Semenov and D. Kirsanov, *Anal. Chim. Acta*, 2018, **1040**, 19–32.
26 F. Armetta, V. MollicaNardo, S. Trusso, M. Saladino, A. Arcovito, E. Cosio, P. Jorio and R. Ponterio, *Spectrochim. Acta, Part B*, 2021, **180**, 106171.
27 C. Scatigno, R. Senesi, G. Festa and C. Andreani, *J. Phys.: Conf. Ser.*, 2020, **1548**, 012030.
28 G. Festa, T. Christiansen, V. Turina, M. Borla, J. Kelleher, L. Arcidiacono, L. Cartechini, R. C. Ponterio, C. Scatigno, R. Senesi and C. Andreani, *Sci. Rep.*, 2019, **9**, 7310.
29 D. H. Hammer and P. Ryan, *Palaeontol. Electron.*, 2001, **4**, 9.
30 C. D. Abernethy, G. M. Codd, M. D. Spicer and M. K. Taylor, *J. Am. Chem. Soc.*, 2003, **125**, 1128–1129.
31 I. Angelini, B. Gratzue and G. Artioli, *EMU Notes in Mineralogy*, 2019, vol. 20, pp. 87–150.
32 S. Saminpanya, C. Saiyasombat, N. Thammajak, C. Samrong, S. Footrakul, N. Potisuppaiboon, E. Sirisurawong, T. Witchanantakul and C. Rojviriya, *Sci. Rep.*, 2019, **9**, 16069.
33 R. B. Scott, A. J. Shortland, P. Degryse, M. Power, K. Domoney, S. Boyen and D. Braekmans, *Glass Technol.*, 2012, **53**, 65–73.
34 P. Degryse, R. B. Scott and D. Brems, *Perspective*, 2014, (2), 224–238.